Advances in Neuromagnetic Instrumentation and Studies of Spontaneous Brain Activity

Samuel J. Williamson,* Lloyd Kaufman*

Summary: Rapid progress in neuromagnetic technology has been achieved during the past two years with the introduction of a method for accurately indicating magnetic sensor locations with respect to a head-based coordinate system and the advent of refrigerator-cooled sensors and larger arrays of sensors. These make possible the real-time monitoring of evoked activity at several widely separated locations over the scalp, thus revealing sequential activity in, e.g., sensory-motor tasks. Arrays of magnetic sensors also provide sufficient information to locate the sources of spontaneous activity, such as alpha rhythm. The locations of discrete generators (alphons) of individual alpha spindles is now possible with an array of 14 sensors. Mapping techniques with a 5-sensor system have revealed preferential suppression of alpha activity within certain regions of the occipital lobe to tasks involving mental comparisons of abstract figures. These studies provide evidence that the machinery of visual cortex is involved in mental imagery.

Keywords: Neuromagnetism; Magnetic sensor; SQUID; Alpha rhythm; Mental imagery

Introduction

One of the important features of neuromagnetic methodology has been an emphasis on the importance of characterizing neuronal sources as distinct from the magnetic fields or electric potentials they produce. The importance of this approach can be traced to the first observations of somatosensory evoked fields (Brenner et al. 1978). It was reinforced by the observation in auditory studies that when the observed field strength (and location of neuronal activity) of a steady-state response varies with tone frequency, neuronal response strength does not (Romani et al. 1982). This suggests that the neuronal population responding to each tone, ranging from about 100 Hz to 5,000 Hz, is essentially the same size. Thus we learn new principles of functional organization by focusing on properties of the source.

Hand in hand with this point of view is an emphasis on quantitative analysis and accuracy in recording the positions of the sensors, in order to locate neuronal sources accurately. Many researchers in neuromagnetism have discarded the tape measure as a means of determining sensor positions with respect to reference points on the scalp. Even mechanical devices that accurately position the sensor with respect to the bed or chair supporting the subject (Williamson et al. 1984) are giving way to newer technology. Accuracy bettering 2 mm for the position of a sensor with respect to the subject's head can be achieved consistently by using a transmitter mounted on the dewar containing the magnetic sensors and a set of three receivers on the subject's head, held by a headband (e.g., the PPI system of Biomagnetic Technologies, Inc., San Diego). Such procedures can locate the cortical source of the 100-ms component of an auditory evoked response with an accuracy of better than 3 mm (Yamamoto, Williamson, Kaufman, Nicholson, and Llinás 1988).

Head-Based Coordinate System

Determining sensor positions as well as orientations with millimeter precision almost requires that distances across the scalp be abandoned as the reference system for

*Neuromagnetism Laboratory of the Departments of Physics and Psychology and Center for Neural Science, New York University, New York, New York, USA.

Accepted for publication: October 31, 1989

Correspondence and reprint requests should be addressed to Dr. S. J. Williamson, Neuromagnetism Laboratory, Department of Physics, 2 Washington Place, New York University, New York, NY 10003, USA.

This work was supported in part by Air Force Office of Scientific Research Grants AFOSR-84-0313, F49620-88-K-0004, and F49620-86-C-0131. We thank Dr. Jia-Zhu Wang for invaluable help with software development, Dr. D.S. Buchanan for calibrating the sensors, Dr. C. Salustri for helpful advice, and P. Fusco for technical assistance.

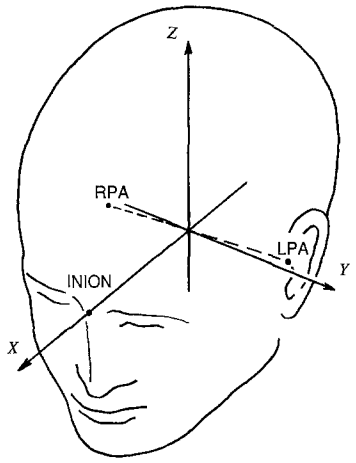

Figure 1. Head-based coordinate system with axes x, y, and z. The orientations of the mutually perpendicular axes are defined in terms of the positions of the left periauricular point (LPA), right periauricular point (RPA), and nasion (NA) as explained in the text. The x-axis passes through the nasion, but in general the y-axis does not pass through the periauricular points.

expressing positions. We have defined a set of Cartesian coordinates that in practice seem most useful because it is prescribed in terms of the nasion and periauricular points. Thus it has a natural relationship to the conventional 10-20 system defining electrode positions on the scalp. The origin of this head-based coordinate system is defined to be exactly midway between the periauricular points (Figure 1). The x-axis of the Cartesian system is a line that extends from this origin through the nasion. The z-axis is defined as the line that extends upward from the origin, oriented perpendicular to the plane defined by the x-axis and the line passing through the periauricular points. The z-axis emerges from the scalp in the general vicinity of the vertex (note that the vertex itself plays no role in the definition of the z-axis). The y-axis is defined as the line that extends toward the left from the origin, oriented perpendicular to the plane defined by the x-axis and z-axis. The y-axis emerges from the scalp in the general vicinity of the left periauricular point. Note that the y-axis in general is not parallel to the line between periauricular points. The coronal plane containing both y- and z-axes is fixed by the positions of nasion and mid-point between periauricular points. We take this to be more anatomically significant than the exact placement of the outer ears. For instance, if the left ear should lie posterior to the right ear, the y-axis emerges anterior to the left periauricular point.

Such a head-based coordinate system serves to reference both the position and orientation of each magnetic sensor being used. Moreover, by using a stylus attached to a receiver it is possible to not only register positions of the PPI receivers relative to the head-based coordinate system but also obtain a digitized image of the shape of the head in the same coordinate system. This is particularly useful if MRI is not available to determine the curvature of the skull when using standard algorithms to deduce the locations of neuronal sources from magnetic data (Cuffin et al. 1977; Williamson et al. 1981; Hari and Ilmoniemi 1986; Williamson et al. 1987). We turn in the next section to describe a recent advance in sensor technology, which provides advantages not found in previous neuromagnetic systems.

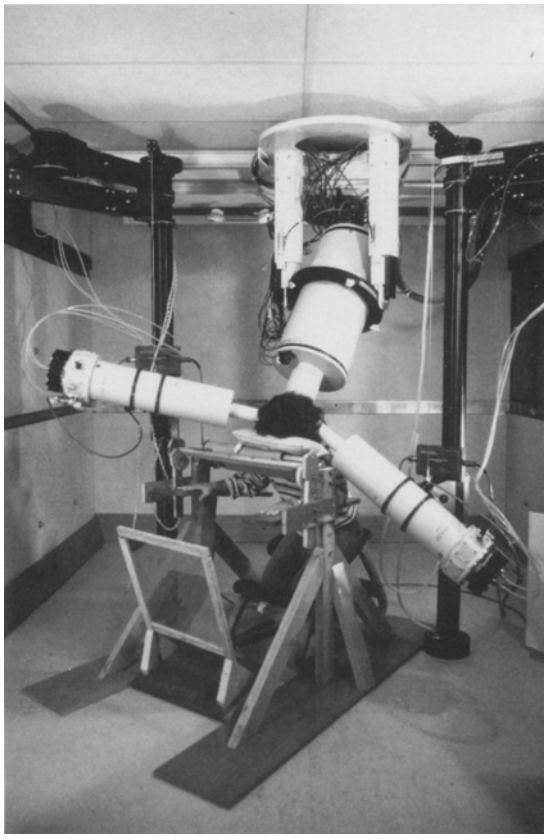

Figure 2. Two CryoSQUIDs (small dewars on the left and right) shown here with a conventional five-sensor system (larger dewar supported from the ceiling) are positioned near a subject in a magnetically shielded room. Each CryoSQUID is supported by an individual tripod gantry permitting horizontal and vertical adjustment as well as positioning in any orientation. Flexible tubing provides high-pressure helium supply and low-pressure return for the refrigerators.

CryoSQUID

Conventional SQUID-based magnetic sensors rely on a reservoir of liquid helium of several litre volume to maintain a low-temperature environment for the super-

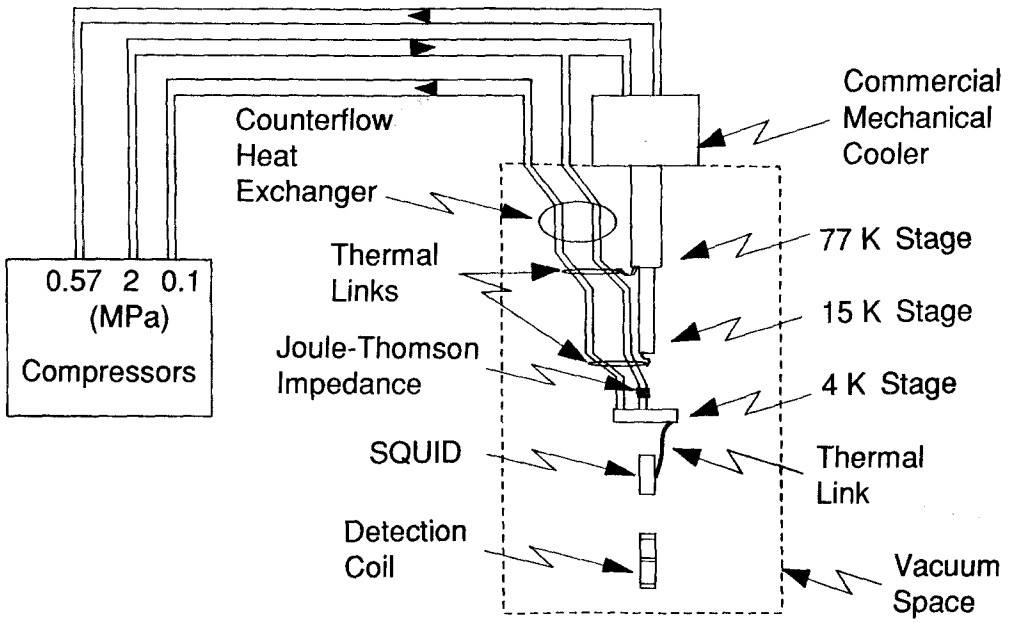

Figure 3. Mechanical cooler (Gifford McMahon cycle) and Joule-Thomson cycle in a CryoSQUID operate from a common feed pressure of 2.3 MPa (megapascal) provided by a commercial compressor. The return at 0.6 MPa from the GM cooler is fed directly to this compressor, but the lower level return of 0.1 MPa from the JT cooler is first enhanced to 0.6 MPa by a second compressor. (From Buchanan, Paulson, and Williamson, 1988)

conducting components. A typical evaporation rate is 3 litre each day. Such a system requires refilling approximately every three days, entails waste of helium, and may be tipped up to only 45 degrees from the vertical, thus imposing a constraint on neuromagnetic measurements. Special dewars with canted tail surfaces and detection coils have been designed to overcome this problem, but still do not allow a full range of measuring positions (Knuutila, Ahlfors, Ahonen, Hällström, Kajola, Lounasmaa, Vilkmanand Tesche 1987). The recent development of a system called "CryoSQUID" based on refrigeration with helium gas virtually elminates these limitations (Buchanan, Paulson and Williamson 1987). CryoSQUID has a completely closed system so it conserves helium and can be oriented in any direction, including upside down. On the other hand it is not an efficient system, requiring several kilowatts of electrical power for a set of compressors, as well as cooling water.

Two single-channel CryoSQUIDs have been installed in a magnetically shielded room at New York University (Figure 2). Refrigeration depends on the fact that helium remains a gas at temperatures as low as 4.2 kelvin (K) at atmospheric pressure. Therefore, cooling cycles were considered that make use of the fact that gaseous helium cools when it is allowed to rapidly expand at a sufficiently low temperature. The final choice was a cascaded sequence of two refrigerators, one that achieves a stable temperature of 15 K and a second that cools from there to 4 K. As illustrated by the diagram in Figure 3, the first stage is a commercial mechanical device, based on the Gifford-McMahon (GM) refrigeration cycle, where a displacer, or free piston, is moved back and forth in a cylinder by alternating high and low pressure gas connections controlled by valves at room temperature. Helium gas passes to and from the dewar by flexible plastic hose, an arrangement which avoids mechanical vibrations of the kind that may be introduced by a mechanical linkage, as used by Zimmerman and Radebaugh (1978) for a Sterling cycle cryocooler. The Sterling cycle had been chosen for the earlier version of a cryocooler because it is more efficient than the GM cycle. The displacer in the present GM cryocooler has a stepped design, so that at the bottom of its upper and lower sections the temperatures are 77 K and 15 K respectively.

Supported from the bottom of the GM stage is a second refrigerator based on the Joule-Thomson (JT) effect. High-pressure helium gas is provided to a chamber having a small hole in one wall (small enough that high pressure can be maintained without loosing the gas through the hole too rapidly). Cooling comes as the gas emerges from the other side of the hole into a chamber of much lower pressure. The cooling rate of this JT stage is sufficient to actually condense some of the helium. The uncondensed helium gas is drawn out of this second chamber by the input of a compressor. For simplicity, this compressor boosts gas pressure to the level of the gas returning from the GM stage. All the gas from both cycles then passes through another compressor, to

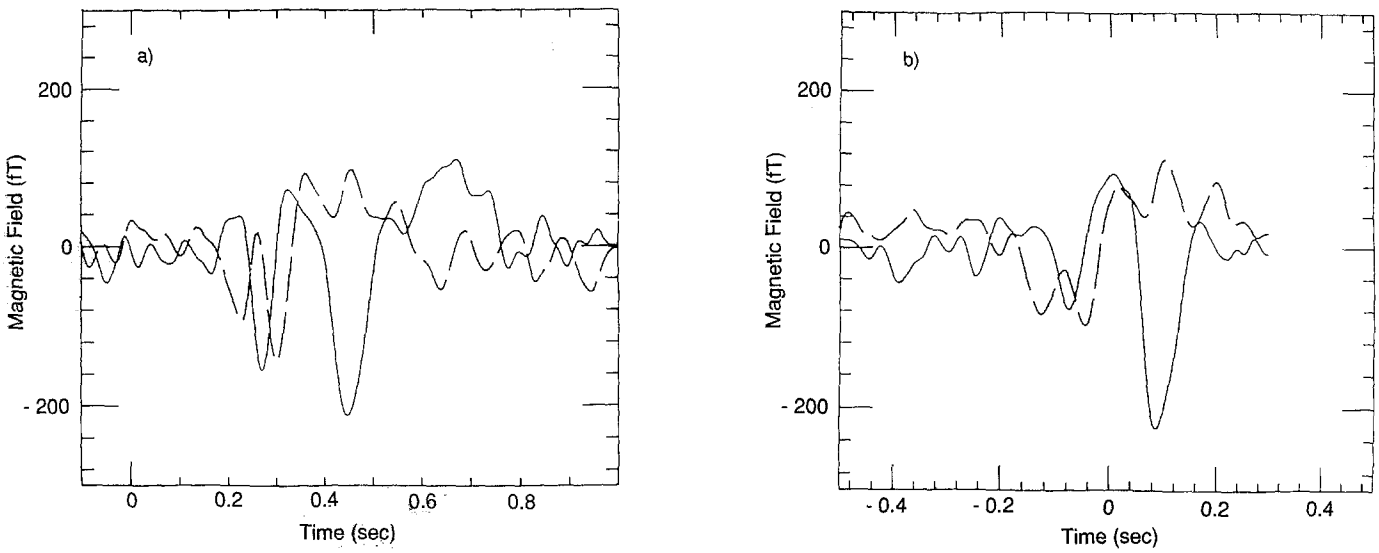

Figure 4. (a) Observed fields in the two CryoSQUIDs when 75 responses are averaged with respect to onset of the visual stimulus. **(b)** The same data when averaged with button press as the time origin. Broken line describes the output from a sensor placed over occipital scalp, and solid line from a sensor placed over the central sulcus. (From Klemic, Buchanan, and Williamson 1989).

achieve the value of high pressure that was chosen for a common input to both the GM stage and JT stage.

A major benefit of collecting in the JT stage a small volume (about 30 cm^3) of helium liquid is that it has a very high specific heat at such low temperature - much greater than that of typical solid construction materials. Therefore, the liquid helium serves as a thermal reservoir, absorbing incoming heat without suffering an appreciable increase in temperature. This provides a very stable temperature for SQUID operation. (Buchanan, Paulson, Klemic and Williamson 1989).

A valve motor controlling the sequence of high and low pressure applied to the GM displacer is mounted outside the shielded room for each CryoSQUID. Residual vibrations from the movement of the displacer in the GM cooler introduce magnetic noise. But since it is time-locked to the motion, a simple computer can be used to register a template and subtract this from the data in real time, removing all detectable noise of refrigerator origin. Cooling from room temperature is achieved after 20 hours simply by starting the compressors.

The reservoir of liquid helium is important for another reason as well. Movement of the displacer of the GM stage, as well as gas passing through the tubing, produces acoustic noise which has proven impossible to eliminate. When this noise must be reduced, as when performing studies with auditory stimuli presented by a loudspeaker, the system can be operated in an "intermittent" mode in which the GM cycle is shut down and the JT flow is reduced. The residual evaporation of helium in the reservoir provides the sole means of countering the residual heat leaking in from outside. If neuromagnetic studies are carried out over a period of 2 - 3 minutes, followed by a similar time of renewed refrigeration, the procedure can be extended for several hours. The whole operation is computer controlled.

A more extreme case is the "one-shot" mode, in which refrigeration is terminated altogether, and 20 minutes of operation is possible before all the helium is evaporated. This system has most recently been in continuous operation for two months without failure, other than stoppages due to human error.

Distribution of Activity: Sensory-Motor Task

One advantage of the pair of CryoSQUIDs was demonstrated recently in a pilot study of spatially distributed activity in the human brain (Klemic et al. 1989). A subject was instructed to press a button with his left index finger when a spot of light appeared on a screen before him. The visual stimulus was a circle of 0.5 deg diameter presented in the lower-right visual field, of 4 ms duration and 1.2 s interstimulus interval. One CryoSQUID was positioned over the left occipital scalp to record activity of visual cortex, (about 3 cm above and

2 cm to left of the inion), and the other was placed over the Rolandic fissure of the left hemisphere at a position known from earlier studies to be where field extrema of both motor and somatosensory areas lie (Okada, Williamson and Kaufman 1982). In this way neuronal activity of motor cortex could be observed prior to button press, and activity of somatosensory cortex would appear following the press.

Results shown in Figure 4a depict the signals when 75 epochs are averaged with respect to onset of the visual stimulus. The two CryoSQUID outputs reveal that strong activity is first observed over occipital scalp, with a latency of about 100 ms. This is followed about 50 ms later by a strong field detected by the second CryoSQUID over the Rolandic fissure. Subsequently contact is made by the reaction time button, and about 75 ms later another strong field of opposite polarity is observed over Rolandic fissure. This illustrates the sequence of visual processing, initiation of activity in motor cortex, and subsequent feedback to somatosensory cortex.

The time relation between these components and the subject's reaction time can be determined another way by averaging the same data with the moment of button contact as the time origin. Figure 3b shows that the moment of peak field over the Rolandic fissure for this realigned average occurs 74 ms prior to the button press, and the subsequent peak occurs 86 ms following button press. These intervals are consistent with the indentification of the first being associated with neuronal activity of motor cortex and the second with activity of somatosensory cortex. The latter reflects efferent input from proprioceptors involved in muscle flexation, perhaps with contributions from pressure on the finger tip from the button.

We note also that the delay between peak activity in visual cortex and motor cortex is 51 ms. This means that the time interval between peak activity in visual cortex and overt reaction is 125 ms, in good agreement with the value of 115 ms obtained for the same subject a decade earlier using steady-state responses to determine the latency of visual cortex response (Williamson, Kaufman and Brenner 1978).

It is interesting to note that in the realigned average the amplitude of the motor peak is diminished relative to the average with respect to stimulus presentation, while all other peaks are about the same. This suggests that jitter in the reaction time is related primarily to variability between motor activity and button press, rather than the interval between responses of visual and motor cortex. This variability may well be due to variability in executing the press. It is well-known that button release introduces less variance in reaction time measures than button press.

Locating Sources of Alpha Spindles

Alpha activity is commonly defined as electrical fluctuations between 8 and 13 Hz that can be detected on the occipital scalp and are attenuated by visual stimuli. While projections from brain stem play a role in its generation (c.f. Steriade and Llinás 1988), evidence for the cortical origin of these electrical signals has been obtained from studies of potentials at various depths within the cortex of animals. Lopes da Silva and van Leeuwen (1978) suggest that alpha sources originate in different epicenters from which activity spreads across cortex in several directions. Previous magnetic studies on humans of the covariance between the EEG and magnetic recordings with a single sensor indicate sources deep within the occipital lobe (Carelli, Foglietti, Modena and Romani 1983). Studies with a four-sensor system (Vvedensky, Ilmoniemi and Kajola 1986) indicate that there are time series of the rhythm lasting for typically 1 sec during which the oscillation period is constant. We call such a time series a spindle, whether or not it occurs in the sleeping state. Ilmoniemi, Williamson, and Hostetler (1988) using a 14-sensor system found that the magnetic field pattern during a spindle appears relatively stable, indicating that its source is a specific configuration of neurons. Moreover, an analysis of the time-invariant spatial pattern based on a 14-dimensional signal space indicates it is possible to distinguish between most of the source patterns of the observed spindles. In other words, the human alpha rhythm represented by the spindles is generated by a large number, or possibly a continuum, of different source configurations.

Williamson, Wang, and Ilmoniemi (1989) have developed a technique to determine the locations in the human brain of these sources and to characterize the orientation and strength of their equivalent current dipole moments. Measurements were carried out at the Center for Neuromagnetism, located at Bellevue Hospital of the New York University Medical Center. Two dewars, each containing seven dc-SQUID sensors (Biomagnetic Technologies, Inc.) were positioned over the left and right occipital areas to record magnetic activity. The detection coils were second-order gradiometers with 1.5-cm diameter and 4-cm baseline, and the sensor noise level was about 20 $fT/Hz^{1/2}$ for most channels, while one or two exhibited noise as high as 50 $fT/Hz^{1/2}$. Individual sensors were calibrated with a relative accuracy of better than 1%. The positions of each dewar, and in turn the sensors within them were determined by the PPI. With the subject prone and alert, recordings within the bandwidth 0.5-50 Hz were made for 16-sec epochs of spontaneous activity with eyes closed. The total level of instrument and subject noise

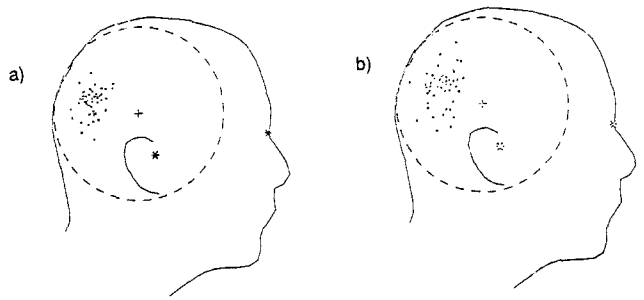

Figure 5. Sagittal views of deduced positions for current dipoles representing neuronal sources that produce spindles with (a) at least one field extremum lying within the area of a probe and (b) neither extremum lying within the area of a probe. Nasion and periauricular points: * ; center of sphere model for posterior head: + ; subject: SW. (From Wang, Williamson, and Ilmoniemi, 1989)

was determined with eyes open. Data were digitally filtered in the bandwidth 8-13 Hz, and a computer routine was used to spot those segments of the time-series where the rms amplitude within the middle 12 seconds of the epoch significantly exceeds the noise level.

A spindle was defined by a time-series where signals in all the sensors are coherent and can be attributed to a single source. The criteria were: (1) the peak rms amplitude averaged across 14 sensors exceeds 500 fT; (2) the mean amplitude exceeds 200 fT for the duration of the spindle; (3) the period between zero crossings is stable to within 5% throughout the duration; and (4) field polarity reverses between the two probes, to ensure that the source lies somewhere between them. Measurements over many days produced on the average 1-3 spindles meeting the criteria during each 12-second analysis period. Visual inspection of our time-series showed on the order of 5 times more spindle-like features that did not meet these criteria.

By positioning the probes so that field extrema of the individual spindles are close by, the source positions in three dimensions can be determined without need to move the dewars. The accuracy of this "fixed position" technique when probes are placed directly over the extrema has been analyzed by Costa Ribeiro, Williamson, and Kaufman (1988), who considered the cases of a single probe with 5 or 7 sensors and two probes with 7 sensors each. However, this is the ideal situation, since determining the positions and fields of the two extrema is sufficient to determine all 5 dipole parameters (Williamson and Kaufman 1981). If both extrema are not within the areas of the probes, accuracy in location greatly diminishes. To ensure accuracy in locating each source, it was important to achieve a high signal-to-noise ratio, because only a small area of the field pattern is measured. The best estimates for the 14 detected amplitudes of a spindle were obtained from elements of the covariance matrix computed across the time-series recorded by the sensors. The set of amplitudes was used to determine the location of the current dipole best representing its source, using a minimum chi-square criterion. The subject's head was modeled as a sphere, whose center of curvature was determined by digitizing the shape of the occipital and parietal areas of the scalp using PPI and determining the best-fitting sphere in the least-squares sense. For analyzing magnetic field data, this head model is equivalent to a set of concentric spherical shells of differing conductivity.

Results

Preliminary studies indicated that strongest spindle amplitudes were detected with the probes placed over right and left occipital scalp, about 4-8 cm above the inion and displaced symmetrically by about 6-8 cm to left and right of the midline. Signals were generally very weak directly over the midline or farther than 9 cm to either side of the midline, in agreement with measures of relative covariance (Carelli et al. 1983; Chapman et al. 1984). Strong alpha rhythm generally produced field extrema of opposite polarity over left and right hemisphere, displaced several centimeters from the midline, indicating that the corresponding sources lie near the midline. Each source was modeled by a current dipole, so its center of activity could be characterized by 5 parameters specifying location, orientation in the plane tangent to the sphere, and strength. Spindles that met the criteria stated above have sources that lie much shallower and closer to the midline than the average positions estimated on the basis of relative covariance measurements (Carelli et al. 1983; Chapman et al. 1984).

The variety of dipoles for a given subject was so diverse that very few of the spindles provided extrema that simultaneously appeared within the areas of the two probes. This remained true when the probes were placed at various asymmetrical positions over left and right hemispheres with one further from the inion or midline than the other. The deduced positions for a set of about 100 sources in one subject are shown in Figure 5, where those providing an extremum within the area of at least one probe (Figure 5a) are compared with a nearly equal number whose extrema lie outside both probes (Figure 5b). The greater scatter in the latter case is due in part to lower accuracy in localization. The uncertainty in posi-

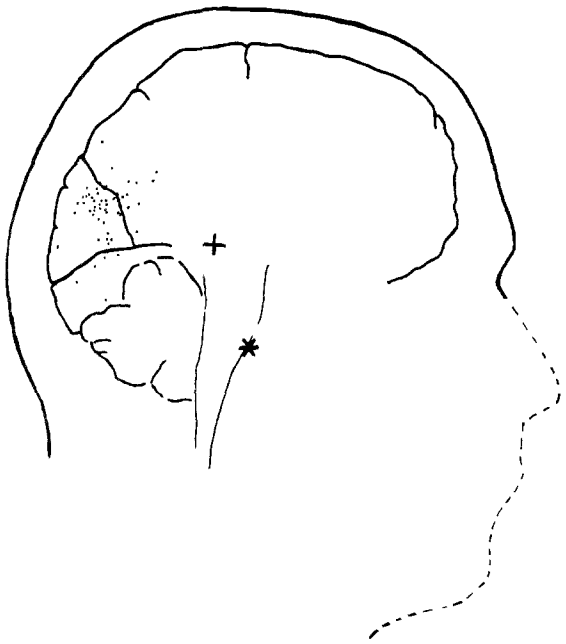

Figure 6. Positions of spindle sources of Fig. 5a, shown in relationship to cortical topology of the subject's brain as obtained from MRI scans.

tion (95% confidence) for the former case is typically about 0.8 cm in radial position and 1.3 cm in distance above the calcarine fissure.

Source positions for this subject were compared with anatomical features obtained from magnetic resonance images. A method was used to reference positions on the images to PPI coordinates with an accuracy of better than 4 mm. Figure 6 shows data from Figure 5a superimposed on tracings of the parieto-occipital fissure, calcarine fissure, and exposed cortical surface near the midline. The fissures were displaced in left and right hemispheres, but by no more than about 1 cm. Figure 6 indicates the average of the hemispheres at the midline. Spindle sources are concentrated in the region of the parieto-occipital and calcarine fissues. Most sources lie within 2 cm of the midline. Similar results were obtained for a second subject.

The deduced orientations of the current dipoles were generally within 30 deg of the longitudinal fissure. When probes were placed on either side of the midline so the line joining them makes an angle of 45 deg or less with the midline, spindles meeting the criteria could not be detected. This justifies our primary reliance on data obtained with the probes placed above the inion at the same distances, or at distances differing by no more than 5 cm.

Since extracranial magnetic fields as measured in this study arise from intracellular currents, the source of the field most likely is an aligned population of cortical neurons. The most conspicuous preferentially aligned population is that of the pyramidal cells. These are aligned perpendicular to the cortical laminae, so in the parieto-occipital and calcarine fissures the current dipole representing each source would be largely tangential to the scalp, and nearly parallel to the longitudinal fissure. This corresponds to our magnetic observations. However, if the portion of visual cortex forming the walls of the longitudinal fissure were also to produce spindles, we would expect by this reasoning to find some dipoles aligned perpendicular to the fissure. We have not detected any dipoles with that orientation. Therefore, the portion of visual cortex within the longitudinal fissure appears to be devoid of alpha activity.

The deduced values for source strengths also prove interesting. The distribution of current dipole moment for about 100 sources was remarkably sharp, with a typical rms current dipole moment of about 40 nA-m and half width of the distribution at half peak of about 20 nA-m. The narrowness of the distribution argues that this cortical excitation involves about the same number of neurons no matter where it occurs in the occipital area. The term alphon was suggested to denote this unitary excitation (Williamson et al. 1989).

Values for alphon dipole moments are sensitive to the choice for the center of curvature of the sphere introduced to model the posterior head. If the midpoint between the periauricular points is (incorrectly) used instead of the center of curvature for the scalp, the deduced source positions lie relatively closer to the scalp than the center, so the deduced rms dipole moment for an alphon decreases by about a factor of 2. Alphon positions, however, are shifted by less than 5 mm.

An alphon moment of 40 nA-m is consistent with the average source strength deduced from relative covariance measurements (Chapman et al. 1984) and is only an order of magnitude greater than a typical sensory evoked response. Considering estimates for postsynaptic currents in pyramidal cells, an area of cortex of only a few square millimeters, corresponding to 10^5 coherently active pyramidal cells, may be required to account for an alphon. This area is an order of magnitude smaller than values deduced on the basis of the cited relative covariance measurements (Chapman et al. opcit), which rely on interpretations of current source density analysis in cortex to determine typical values of current density. But it is consistent with electrophysiological studies (Lopes da Silva and van Leeuwen 1978). However at this time the possibility cannot be ruled out that alphons are wide-spread excitations, with the deduced source location for each representing the center of activity.

The picture that emerges from this work is that magnetic alpha rhythm arises from many discrete sources - alphons - oscillating one after another and occasionally overlapping temporally, if not spatially. Alphons giving rise to the activity observed in this study are clustered

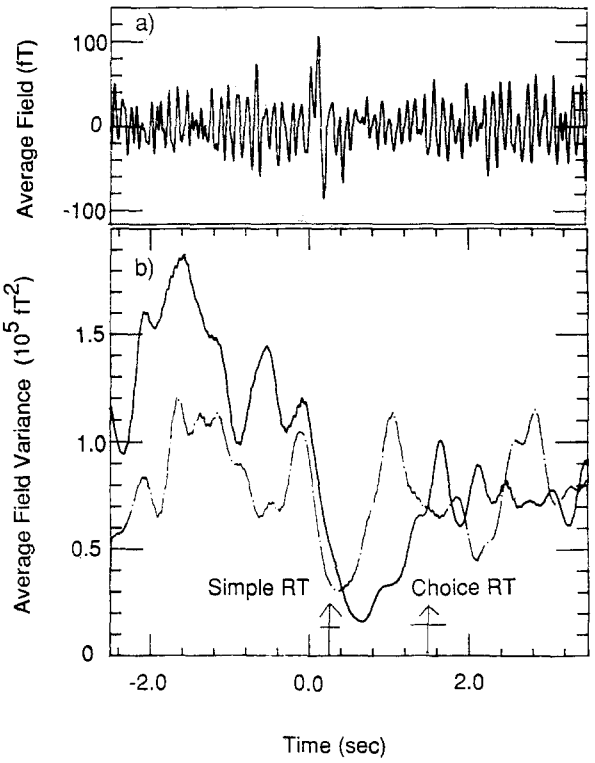

Figure 7. (a) Averaged visually evoked response, with the onset of figure presentation at the time origin. This evoked field is a grand average of 10 groups of 30 trials for all 5 sensors, as it was impossible to obtain a sharply defined evoked field averaging only 30 trials. **(b)** Representative time dependence within the same period for the variance within the alpha band, averaged across 30 epochs. Solid line is the SRT condition, broken line is the CRT condition. Respective average reaction times are indicated by arrows. (From Kaufman, Schwartz, Salustri, and Williamson, 1990)

near the midline, extending to a depth of several centimeters beneath the scalp. They are found predominantly in parieto-occipital and calcarine fissures, with no evidence of activity in the longitudinal fissure.

Alpha Suppression Related to a Cognitive Task

When subjects are in a resting but alert state, alpha activity (8-13 Hz) predominates in the spontaneous EEG. It has been reported (Kaufman and Locker 1970; Pfurtscheller and Aranibar 1977; Pfurtscheller 1987) that alpha activity diminishes coinciding with presentation of visual stimuli and that the duration of this alpha supression is much longer than that of the classic evoked response. Kaufman, Schwartz, Salustri and Williamson (1990) have recently reported that MEG activity during a visual memory task shows a dramatic amplitude reduction in the alpha range lasting 500 to 2000 msec, following which the amplitude recovers despite continuous visual fixation on the display.

As just illustrated, alphons may be found distributed across a broad area of cortex, suggesting that alpha suppression can be localized specifically to visual cortex. To test this hypothesis a combination of two classic paradigms were used: Sternberg's memory matching task (Sternberg 1969) and Shepard's mental rotation task (Shepard and Metzler 1971). Both tasks require a search of memory for representations of visual images, and performance in each case is indexed by systematic differences in choice reaction time (RT). Both alpha suppression and averaged responses were observed. The effect will be illustrated here with results from one 41 year old male subject. These results are similar to those obtained with 6 other subjects.

Methods

The subject, seated on a chair in a magnetically shielded room, maintained fixation on a small cross and viewed a sequence of three irregular polygon figures on a dark background in the lower right quadrant of his visual field. Each figure was seen outlined in white for 1 sec followed by a 300 msec dark interval; 3.0 sec after the disappearance of the last image a fourth "probe" figure was presented for only 100 msec. In one block of trials ("choice reaction time", CRT) the subject pressed one of two buttons after seeing the probe, indicating whether it belonged in the memory set or was new. In a second block of trials ("simple reaction time", SRT) the subject simply had to press one button as soon as he saw the probe. In this task, the subject still had to attend to the whole sequence of visual figures in order to know which one required a response. Each block consisted of a sequence of 30 trials.

The component of the magnetic field normal to the subject's head was recorded over posterior and parietal areas at 65 different locations by means of a 5-channel SQUID system The outputs of the SQUIDs were bandpassed between 0.1 - 50 Hz and recorded on computer disk. Each recording epoch lasted 7 sec, beginning 3 sec prior to and extending 4 sec following the onset of the probe. Visual evoked fields were extracted after digitally filtering the MEG record between 1 and 20 Hz and then averaging over the 30 recording epochs (Figure 7). Alpha activity was isolated by filtering the record between 8 and 12 Hz, and computing the variance across the 30 trials in each block as a function of time for each SQUID channel. This variance is the mean square field (power) with the average evoked response removed. Temporal changes in the variance averaged across epochs are due to changes in amplitude, not to coherence

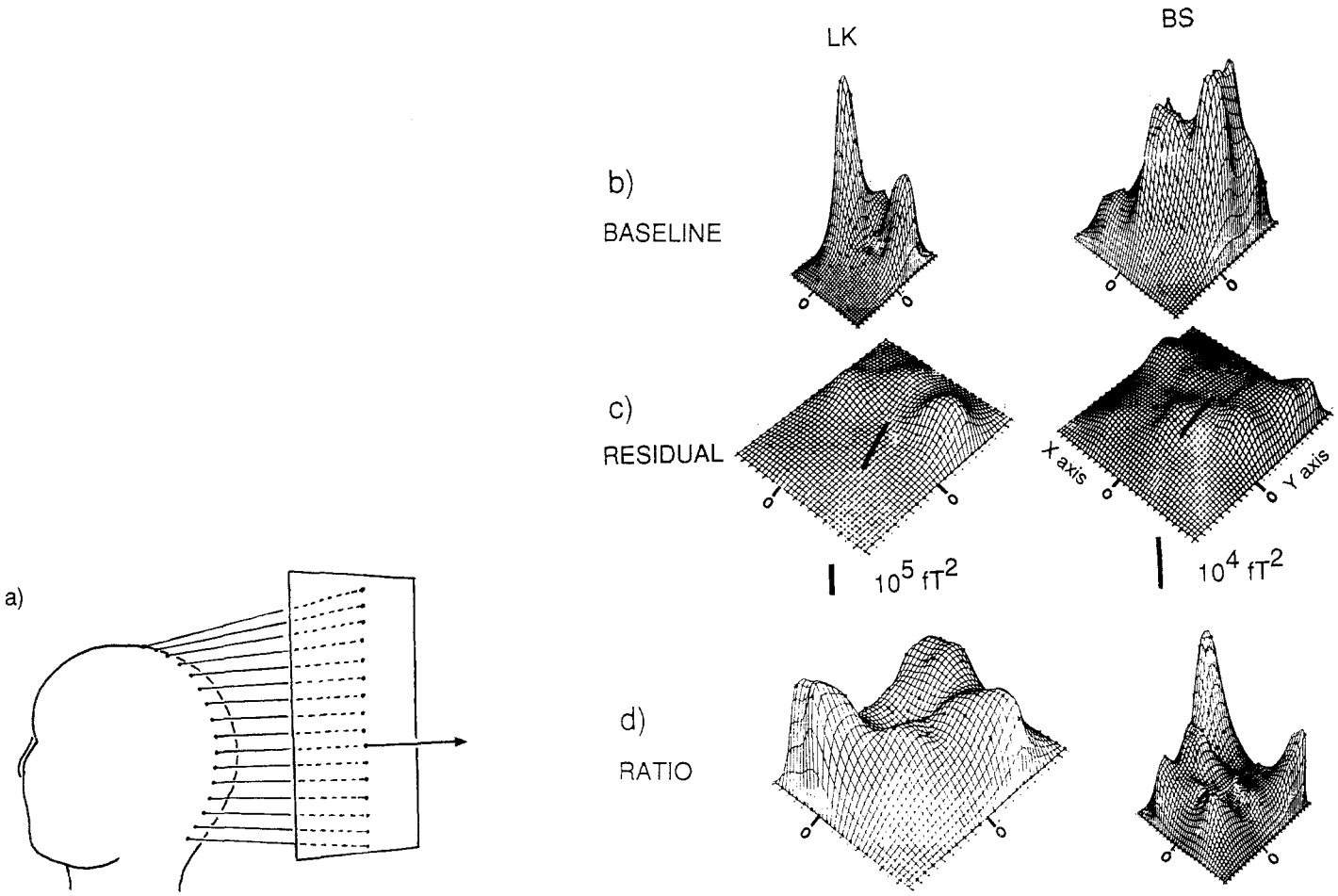

Figure 8. (a) Distribution of average alpha power across the posterior scalp portrayed by an azimuthal equal distance projection. Equal distances across the surface of a spherical representation of the head from the center of projection are mapped onto equal distances across a flat plane. **(b)** Distribution of average baseline alpha, defined as the average alpha power observed within a 200 msec interval 100 msec prior to presentation of the visual probe in the CRT condition. **(c)** Distribution of alpha power averaged over a 100 msec interval centered on the moment of maximum suppression. Dark, solid line represents the midline. **(d)** Distribution of the ratio of residual to baseline alpha, which defines the relative residual alpha. (From Kaufman, Schwartz, Salustri, and Williamson, 1990)

across the epochs. An examination of the time-course of single trial data shows that alpha activity is not time-locked to the stimulus onset.

Results

During the performance of visual memory-search tasks (Figure 7), MEG power in the alpha band exhibits a systematic reduction below the level observed prior to presentation of the probe (baseline level). For SRT trials, suppression lasts for only about 500 msec, beginning at the time of probe stimulus onset. On the other hand, alpha power for CRT trials is sharply suppressed and maintained for about 1500 msec. The duration of evoked responses for both tasks are typical of sensory evoked responses, on the order of 100 msec.

The RT for the SRT task coincides with the minimum of its alpha power curve, about 500 msec after the onset of the probe. Suppression of alpha power for CRT trials is significantly longer, and 1200 msec after stimulus onset the alpha power is only half way through its recovery back to its baseline level. The RT for the CRT task occurs during this recovery phase (Figure 7). The longer duration of the suppression in the CRT task is consistent with the interpretation that the visual cortex is engaged during a search of memory.

The distribution of alpha power over the scalp prior to and following the suppression is quite similar, with a correlation of 0.81 over 65 measured positions ($p < 0.001$). There is less of a similarity in distribution over the scalp during the time of maximum suppression. To characterize the suppression of alpha activity during mental imagery, the magnitude of average alpha power was plotted as a function of position over the posterior scalp

(Figure 8). The average power within a 2 sec interval 200 msec prior to presentation of the probe stimulus represents the baseline, which has a peak in the right hemisphere about 5 cm above the inion and 5 cm to the right of the mid-line. It is important to note that the distribution changes during maximum suppression, with overall reduction in activity most pronounced in the vicinity of the midline. Figure 2d represents the proportional change in alpha power, or the ratio of c) to b) at each location over the scalp. If the suppression of alpha were global and uniform, the topography of this relative residual alpha would be flat. Instead, it is greatest in a band centered approximately on the mid-line, in the region from above the inion to below the vertex. The pattern of suppression is consistent with changes in neuronal activity of limited extent across the more posterior area of visual cortex.

There are individual differences in local patterns of alpha distribution for three subjects whose fields have been extensively mapped. Individual differences in the strength and distribution of alpha cannot be attributed to differences in skull thickness (Leissner, Lindholm and Petrsen 1970), since thickness of the skull has a negligible effect on magnetic fields. Instead, they must be attributed to underlying brain anatomy and neural function. We note in passing that when alpha is suppressed, beta activity (16-24 Hz) does not show an increase, contrary to some predictions.

These data support the hypothesis that power within the alpha band is systematically reduced during the performance of a mental task involving the matching of memories of visual images. The source of this reduction appears to be in the visual cortex, a finding that is consistent with local cerebral blood flow studies (Friberg and Roland 1985). Although the field pattern of alpha appears to be suppressed over a widespread area on the occipital scalp, a more local pattern of suppression is clearly superimposed on it. Functionally, this suppression is correlated not merely with visual attention, but more specifically with the task of visual memory search, since its duration varies with task and also correlates with RT. We believe the above procedure will prove useful for direct tests of hypotheses about the roles of various areas of the brain during different types of mental acts.

References

Brenner, D., Lipton, J., Kaufman, L. and Williamson, S. J. Somatically evoked magnetic fields of the human brain, Science 199, 1978: 81-83.

Buchanan, D.S., Paulson, D. and Williamson, S.J. Instrumentation for clinical applications of neuromagnetism, In: R.W. Fast (Ed.), Advances in Cryogenic Engineering Vol. 33, Plenum Press, New York, 1987: 97 - 106.

Buchanan, D.S., Paulson, D.N., Klemic, G.A. and Williamson, S.J. Development of a Hybrid Gifford-McMahon Joule-Thomson Based SQUID gradiometer, In: P.Lindquist and A. Johnson, (Eds.), Proceedings of the International Cryocooler Conference, 1988.

Carelli, P., Foglietti, V., Modena, I. and Romani, G.L. Magnetic study of the spontaneous brain activity of normal subjects, Ill Nuovo Cimento 2D, 1983: 538-546.

Chapman, R.M., Ilmoniemi, R.J., Barbanera, S. and Romani, G.L. Selective localization of alpha brain activity with neuromagnetic measurements, Electroenceph. Clin. Neurophysiol. 58, 1984: 569-572.

Costa Ribeiro, P., Williamson, S.J. and Kaufman, L. SQUID arrays for simultaneous magnetic measurements: calibration and source localization performance, IEEE Trans. Biomed. Engr. BME-35, 1988: 551 - 560.

Cuffin, B.N. and Cohen, D. Magnetic fields of a dipole in special volume conductor shapes, IEEE Trans. Biomed. Engr. BME-24, 372-381.

Friberg, L. and Roland, P.E. Localization of cortical areas activated by thinking, J. Neurophysiol. 53: 1985: 1219-1243.

Hari, R. and Ilmoniemi, R. J. Cerebral magnetic fields, 1986, CRC Critical Rev. in Biomed. Eng. 14, 1986: 93-126.

Ilmoniemi, R.J., Williamson, S.J. and Hostetler, W.E. New Method for the study of spontaneous brain activity, In: K. Atsumi, M. Kotani, M. S. Ueno, T. Katila and S. J. Williamson, (Eds.), Biomagnetism '87, Tokyo Denki University Press, 1987: 182-185.

Kaufman, L. and Locker, Y. Sensory modulation of the EEG, Proc. 78th Annual Conv. Amer. Psychol. Assoc., 1970: 179-180.

Kaufman, L., Schwartz, B., Salustri, C. and Williamson, S.J. Modulation of spontaneous brain activity during mental imagery, J. Cognitive Neuroscience, 1990, in press.

Klemic G., Buchanan, D.S., Cycowicz, Y. and Williamson, S.J. Sequential spatially distributed activity of the human brain detected magnetically by CryoSQUIDs, In: S. J. Williamson, M. Hoke, G. Stroink and M. Kotani, (Eds.), Advances in Biomagnetism, Plenum Press, New York, 1989: in press.

Knuutila, J., Ahlfors, S., Ahonen, A., Hällström, J., Kajola, M., Lounasmaa, O.V., Vilkman, V. and Tesche, C. Large-area low-noise seven-channel dc SQUID magnetometer for brain research, Rev. Sci. Instrum., 58, 1987: 2145-2156.

Leissner P., Lindholm, L.-E. and Petersen, I. Alpha amplitude dependence on skull thickness as measured by ultrasound technique, Electroenceph. Clin. Neurophysiol., 29, 1970: 392-399.

Lopes Da Silva, F.H. and van Leeuwen, S. The cortical alpha rhythm in dog: The depth and surface profile of phase, In: M.A.B. Brazier and H. Petsche, (Eds.), Architectonics of the Cerebral Cortex, Raven Press, New York, 1978: 319-333.

Okada, Y.C., Williamson, S.J. and Kaufman, L. Magnetic field of the human sensorimotor cortex, Intern. J. Neuroscience 17, 1982: 33-38.

Pfurtscheller, G. and Aranibar, A. Event-related desynchronization detected by power measurements of scalp EEG, Electroenceph. Clin. Neurophysiol 42, 1977: 138-146.

Pfurtscheller, G. Mapping of event-related desynchronization and type of derivation, Electroenceph. Clin. Neurophysiol

70, 1988: 190-193.
Romani, G.L., Williamson, S.J., Kaufman, L. and Brenner, D. Characterization of the human auditory cortex by the neuromagnetic method, Exp. Brain Res. 47: 1982: 381-393.
Shepard, R.N. and Metzler, J. Mental rotation of three dimensional objects, Science, 220, 1971: 632-634.
Steriade, M. and Llinás, R.R. The functional states of the thalamus and the associated neuronal interplay, Physiol. Revs. 68, 1988: 649-742.
Sternberg, S. Memory scanning: mental processes revealed by reaction time experiments, Amer. Scientist, 57, 1969: 421-457.
Vvedensky, V.L., Ilmoniemi, R.J. and Kajola, M.L. Study of the alpha rhythm with a 4-channel SQUID magnetometer, Med. & Biol. Eng. & Computing 23, Suppl. Part 1, 1986: 11-12.
Williamson, S. J., Kaufman, L. and Brenner, D. Latency of the neuromagnetic response of the human visual cortex, Vision Res. 18, 1978: 107-110.
Williamson, S. J. and Kaufman, L. Evoked cortical magnetic fields, In: S.N. Erné, H.D. Hahlbohm and H. Lübbig (Eds.), Biomagnetism, de Gruyter, Berlin 1981: 353-402.
Williamson, S. J. Pelizzone, M., Okada, Y., Kaufman, L., Crum, D. B. and Marsden J. R. Magnetoencephalography with an array of SQUID sensors, In: H. Collan, P. Berglund and M. Krusius (Eds.), Proceedings of the Tenth Internation Cyrogenic Engineering Conference - ICEC10, Butterworth, Guildford, Surrey, 1984: 339-348.
Williamson, S.J. and Kaufman, L. Analysis of neuromagnetic signals, 1987, In: A.S. Gevins and A. Rémond (Eds.), Handbook of Electroencephalography and Clinical Neurophysiology, Volume 1 Revised,Elsevier, Amsterdam, 1987: 405-448.
Williamson, S.J., Wang, J.Z. and Ilmoniemi, R.J. Method for locating sources of human alpha activity, In: S.J. Williamson, M. Hoke, G. Stroink and M. Kotani, (Eds.), Advances in Biomagnetism, Plenum Press, New York, 1989: in press.
Yamamoto, T., Williamson, S.J., Kaufman, L., Nicholson, C. and Llinás, R. Magnetic localization of neuronal activity in the human brain, Proc. Natl. Acad. Sci. USA 85, 1988: 8732 - 8736.
Zimmerman, J.E. and Radebaugh, R. Operation of a very low-power cryo-cooler, In: J.E. Zimmerman and T.M. Flynn, T.M. (Eds.), Applications of Closed Cycle Cryocoolers to Small Superconducting Devices,NBS Special Publication No. 508, 1978: 59-65.